Temperature memory and resistive glassy behavior of a perovskite manganite

D. N. H. Nam,* N. V. Khien, N. V. Dai, L. V. Hong, and N. X. Phuc
Institute of Materials Science, VAST, 18 Hoang-Quoc-Viet, Hanoi, Vietnam
(Received 8 February 2008; revised manuscript received 1 April 2008; published 4 June 2008)

In this paper we report the observations of long-time relaxation, aging, and temperature memory behaviors of resistance and magnetization in the ferromagnetic state of the polycrystalline $La_{0.7}Ca_{0.3}Mn_{0.925}Ti_{0.075}O_3$ compound. The observed glassy dynamics of the electrical transport appears to have a magnetic origin and has a very close association with the magnetic glassiness of the sample. The phase separation and strong correlation between magnetic interactions and electronic conduction play the essential roles in producing such a resistive glassiness. We explain the observed effects in terms of a coexistence of two competing thermomagnetic processes, domain growth and magnetic freezing, and propose that hole-doped perovskite manganites can be considered as resistive glasses.

DOI: 10.1103/PhysRevB.77.214406 PACS number(s): 72.20.Pa, 72.20.My, 75.47.Lx, 75.50.Lk

I. INTRODUCTION

Glassy systems are well known for their nonequilibrium slow dynamics such as long-time relaxation, aging, and memory behaviors. Although the dynamics of electrons is generally considered very rapid, glassy transport has been observed in various systems including electron glasses in Anderson-insulator film structures,[1,2] a two-dimensional electron system in Si (Ref. 3) and mesoporous Si,[4] ultrathin and granular metal films,[5–7] rare-earth hydrides $YH_{3-\delta}$,[8] and a number of perovskite manganite and cobaltite polycrystalline bulks,[9–12] single crystals,[13–15] films,[16–19] etc. Such nonergodic electron dynamics is obviously not expected in conventional electronic systems; and the underlying physics may not be unique, considering the fact that it can be observed in a variety of materials. As for mixed-valence manganites, $R_{1-x}A_xMnO_3$ (R: trivalent rare earth; A: divalent alkaline element), the slow resistance relaxation and aging phenomena were noticed quite early by Helmolt *et al.*[16] after the discovery of the colossal magnetoresistance (CMR) effect.[20,21] The observed glassy transport has been commonly attributed to the slow evolution of the phase conversions among competing phases coexisting in the material as a result of phase separation. Remarkably, using high-resolution transmission electron microscopy technique, Tao *et al.*[11] observed a dynamic competition between charge-ordered and charge-disordered phases in $La_{0.23}Ca_{0.77}MnO_3$ and related it to the change in the time dependence of the resistivity. However, the authors also suggested that the resistivity relaxation could be a property of the charge-ordered (orthorhombic) phase itself and not related to the phase coexistence. Kimura *et al.*[14] compared the transport and magnetic behaviors of Cr-doped $Nd_{1/2}Ca_{1/2}MnO_3$ with the dielectric phenomena in "relaxor ferroelectrics" and proposed that the system can be viewed as a "relaxor ferromagnet." In addition, Wu *et al.*[13] observed glassy transport in $La_{1-x}Sr_xCoO_3$ cobaltites and specifically ascribed the phenomenon to the dynamics of the sample's spin-glass component.

We report here the observations of long-time relaxation, aging, and memory behaviors of resistivity, which apparently very much resemble the characteristics of spin glasses, in the ferromagnetic (FM) state of the polycrystalline $La_{0.7}Ca_{0.3}Mn_{0.925}Ti_{0.075}O_3$ compound. The resistive glassy dynamics exists in zero magnetic field but is found to be magnetically related. Strikingly, temperature memory behaviors of both resistivity and magnetization are revealed in the ferromagnetic state. We explain the results in terms of two competitive thermomagnetic processes: domain growth and magnetic freezing. We propose that glassy transport is a common behavior of mixed-valence perovskite compounds where phase separation occurs spontaneously and the interplay between magnetism and electrical property is strong; the materials therefore can be considered as resistive glasses.

II. EXPERIMENTS

The $La_{0.7}Ca_{0.3}Mn_{0.925}Ti_{0.075}O_3$ compound was prepared by a conventional solid-state reaction method. Pure ($\geq$99.99%) raw powders with appropriate amounts of La_2O_3, $CaCO_3$, MnO_2, and TiO_2 were thoroughly ground, mixed, pelletized, and then calcined at several thermal processing steps with increasing temperatures from 900–1200 °C sandwiched by intermediate grindings and pelletizations. The product was then sintered at 1300 °C for 48 h in ambient atmosphere. The final sample was obtained after a very slow cooling process from the sintering to room temperature with an annealing step at 700 °C for 5 h. Room-temperature x-ray diffraction measurements showed that the sample is single phase of a perovskite orthorhombic (space group *Pnma*) structure. Redox titration experiments showed no sign of oxygen deficiency or excess. Field-cooled and zero-field-cooled magnetization and four-probe resistivity measurements were carried out in a Quantum Design physical property measurement system (PPMS)-6000. The sample used for resistivity measurements was a $1.9\times1.2\times7.5$ mm^3 rectangular bar that was firmly glued to the PPMS puck to have a good thermal contact but electrically separated from the puck by a sheet of cigarette paper. To reduce Joule heating and current induced effects, a very small dc current $I=100$ nA (corresponding to a current density of 4.4 μA/cm^2) driven in ac mode was used. A low heating and cooling rate of 1 K/min was always chosen for all of the measurements.

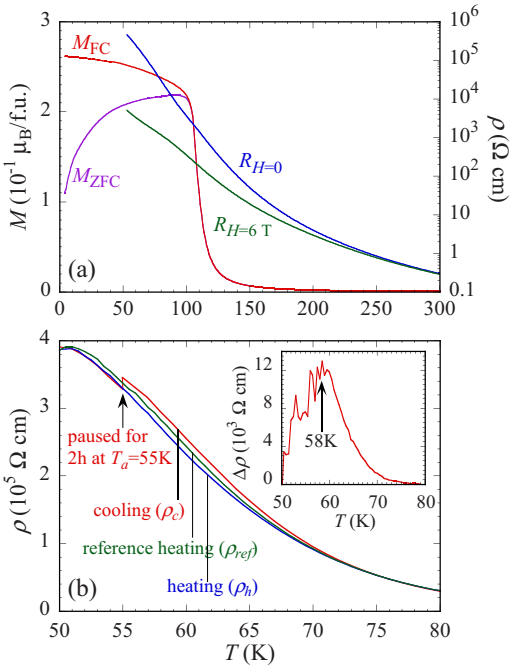

FIG. 1. (Color online) (a) $M_{ZFC}(T)$, $M_{FC}(T)$ (left axis; $H=100$ Oe), and $\rho(T)$ (right axis; $H=0$ and 6 T) of $La_{0.7}Ca_{0.3}Mn_{0.925}Ti_{0.075}O_3$. (b) $\rho(T)$ measured by different protocols: $\rho_{ref}(T)$ was measured on heating following a continuous cooling from 300 to 50 K, $\rho_c(T)$ was recorded during cooling the sample to 50 K with a pause at 55 K for 2 h, and $\rho_h(T)$ was then measured on reheating. The inset of (b) shows the reduced resistivity $\Delta\rho(T)=\rho_{ref}(T)-\rho_h(T)$ that exhibits a maximum at ~58 K.

III. RESULTS AND DISCUSSION

A. Magnetic and transport characterizations

According to the double-exchange (DE) mechanism for mixed-valence manganites,[22] the transfer of an e_g electron between two adjacent Mn ions occurs only when their localized t_{2g} magnetic moments are aligned in parallel, implying that metallic-conducting behavior should come along with a FM state. Nevertheless, manganites are strongly separated systems, so that the ideal DE correlation between magnetism and electrical transport may not be always obtained. While $La_{0.7}Ca_{0.3}MnO_3$ is a typical DE ferromagnet that has a metallic-conducting behavior in the FM phase below $T_c \approx 247$ K, since Ti^{4+} ions do not take part in magnetic couplings, substitution of Mn by Ti destabilizes the network of Mn ions, leading to a deterioration of both DE ferromagnetism and conductivity.[23,24] Temperature dependent magnetizations, $M_{ZFC}(T)$ and $M_{FC}(T)$, and resistivity $\rho(T)$ in Fig. 1(a) show that the $La_{0.7}Ca_{0.3}Mn_{0.925}Ti_{0.075}O_3$ compound is an insulator ferromagnet with $T_c \approx 108$ K (T_c was determined as the temperature at which dM/dT shows a sharp peak in the phase transition region). The insulating behavior in the FM state would suggest that the sample is segregated into metallic-conducting FM regions separated by non-FM insulating boundaries. With decreasing temperature, the resistance increases continuously and goes beyond the limit of our measurement system below 50 K. Under the influence of a magnetic field $H=6$ T, the transport behavior remains that of an insulator but the resistance is strongly suppressed, leading to a negative magnetoresistance, $-MR=(R_{H=0}-R_{H=6T})/R_{H=6T}$, which increases with lowering temperature and reaches up to ~9000% at 50 K. The negative magnetoresistance is probably due to an expansion of the DE FM metallic-conducting regions that is more favored at lower temperatures.

B. Temperature memory and resistive glassy behavior

The $\rho(T)$ data in Fig. 1(a) were measured upon reheating the sample from 50 K following a continuous cooling from 300 K. The $\rho(T)$ curve in zero field is replotted in Fig. 1(b) as a reference heating curve, denoted as $\rho_{ref}(T)$. In other measurements, instead of cooling down the sample continuously directly to 50 K, the cooling was paused at a constant temperature $T_a < T_c$ for a duration time t_a. Interestingly, we observed a clear resistance relaxation that had no tendency to stop even after several hours during the pause, showing a signature of an aging process. The cooling was then resumed to cool the sample to 50 K. A typical $\rho(T)$ curve recorded during this cooling procedure with $T_a=55$ K and $t_a=2$ h are plotted as $\rho_c(T)$ in Fig. 1(b), which shows a step at T_a caused by the aging. Right after reaching 50 K, the temperature was swept back and $\rho_h(T)$ data were collected. Intuitively, curves $\rho_{ref}(T)$ and $\rho_h(T)$ are not the same, indicating a cooling history dependence. By subtracting $\rho_h(T)$ from $\rho_{ref}(T)$ we obtained a temperature dependence of the reduced resistivity, $\Delta\rho(T)$, that shows a maximum at ~58 K [inset of Fig. 1(b)], which is very close to the temperature at which the pause was made. This feature seems to imply that the pause at T_a during cooling was imprinted into the system and can be retrieved on reheating, signaling the presence of a temperature memory effect that was previously observed in magnetic glassy systems.[25–27] As shown in Fig. 2, this memory behavior is verified by a series of measurements where T_a is systematically varied. Henceforth, we refer the measurement of a heating curve following a paused cooling as "memory measurement" (or "memory curve"). In the case where one pause is made, the memory characterized by a maximum of $\Delta\rho(T)$ is then called "single temperature memory" (SME) and $\Delta\rho$ is denoted as $\Delta\rho_{SME}^{T_a}$.

Observations of magnetic glassy behaviors similar to those of canonical spin glasses in DE perovskite cobaltites and manganites have been reported in a number of publications.[28–31] However, although signatures of glassy transport such as slow relaxation and aging were sometimes observed, memory behaviors of resistance have not been explored so far. To confirm the memory behavior in Fig. 1(b), we carried out a series of similar experiments with $t_a=2$ h but various temperatures T_a's; the results are presented in Fig. 2. The maximum of $\Delta\rho_{SME}^{T_a}$ near T_a is reproducibly obtained but strongly suppressed with increasing T_a and finally vanished for $T_a > T_c$; i.e., it is well defined for $T_a=55$, 60, 65, 70, and 75 K, but appears less and less defined with further increasing T_a and becomes unresolvable for $T_a=110$ K. Irrespective of T_a, $\Delta\rho_{SME}^{T_a}$ is strongly suppressed with temperature and basically becomes zero in the paramagnetic state. Although a magnetic field is not required for the observation

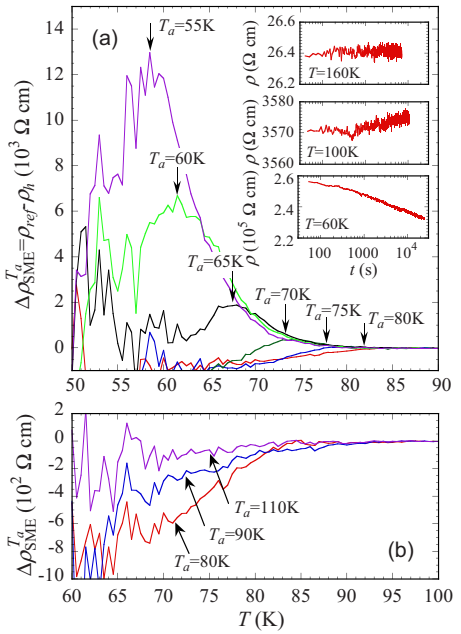

FIG. 2. (Color online) Single temperature memory curves, $\Delta\rho^{T_a}_{SME}(T)$, with different T_a's. (a) $\Delta\rho^{T_a}_{SME}(T)$ curves for T_a=55, 60, 65, 70, 75, and 80 K. The arrows mark the $\Delta\rho^{T_a}_{SME}(T)$ maximum with the corresponding T_a. The insets display $\rho(t)$ curves measured at T_a=60, 100, and 160 K. (b) $\Delta\rho^{T_a}_{SME}(T)$ for T_a=80, 90, and 110 K. The arrows mark the $\Delta\rho^{T_a}_{SME}(T)$ curve with the corresponding T_a.

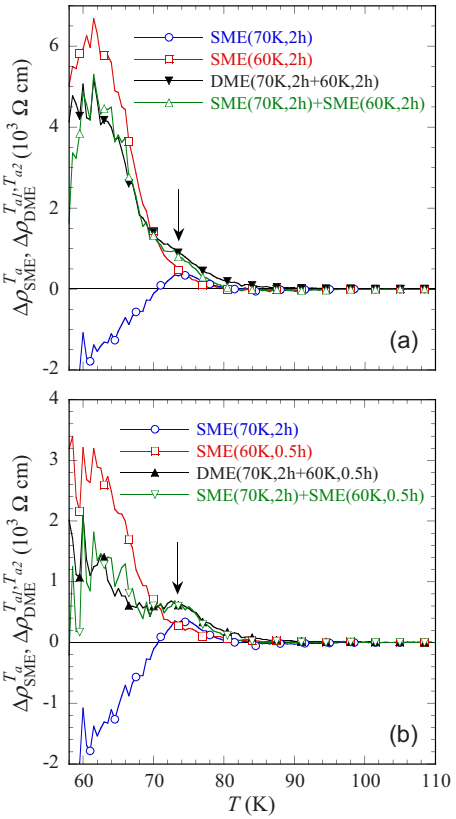

FIG. 3. (Color online) Double temperature memory as a combination of the corresponding single temperature memories, $\Delta\rho^{T_{a1},T_{a2}}_{DME}(T)=\Delta\rho^{T_a}_{SME}(T)+\Delta\rho^{T_a}_{SME}(T)$. The $\Delta\rho^{T_{a1},T_{a2}}_{DME}(T)$ curve shows a maximum near T_{a2}=60 K and a shoulder or cusp (marked by an arrow) near T_{a1}=70 K. t_{a1}=2 h for all measurements. The upper panel (a) is for t_{a2}=2 h; the lower panel (b) is for t_{a2}=0.5 h. Symbols: ○=$\Delta\rho^{70\ K}_{SME}$, □/⊡=$\Delta\rho^{60\ K}_{SME}$, ▼/▲=$\Delta\rho^{70\ K,60\ K}_{DME}$, △/▽=$\Delta\rho^{70\ K}_{SME}+\Delta\rho^{60\ K}_{SME}$.

of this memory effect, these results unambiguously indicate that it is indeed magnetically related. Another noticeable feature is the tendency of $\Delta\rho^{T_a}_{SME}$ at $T<T_a$ to change its sign to negative when T_a approaches close to T_c. Resistivity relaxation curves, $\rho(t)$, measured during the pauses at T_a=60 K ($\ll T_c$), 100 K($\approx T_c$), and 160 K ($\gg T_c$) and plotted in the insets of Fig. 2(a) clearly show a very strong downward relaxation at 60 K, a weaker upward relaxation at 100 K, and no relaxation at all at 160 K. Qualitatively, the changes in both amplitude and sign of $\rho(t)$ are consistent with the variation of the $\Delta\rho^{T_a}_{SME}$ curves. Although the underlying physics is probably different, this behavior is reminiscent of the change in relaxation direction of the field-cooled magnetization in the vicinity of the glass phase transition in spin glasses and random magnets.[26,31]

The results in Fig. 2 clearly demonstrate that the system memorizes the temperature at which an event was made during cooling and recalls it on reheating. To figure out whether the system can memorize separately more than one event in a single cooling (thus yielding a "multiple temperature memory"), we made two pauses with the same t_a=2 h sequentially at T_{a1}=70 K and T_{a2}=60 K in the same cooling process. The corresponding $\Delta\rho$ curve [Fig. 3(a)] shows a large maximum near 60 K and a small shoulder around 70 K, indicating a "double temperature memory" (DME) behavior. Moreover, this DME is in fact a combination of the two SME's at the corresponding T_a's; i.e., the summation of the two SME curves with T_a=60 and 70 K, $\Delta\rho^{60\ K}_{SME}(T)$ and $\Delta\rho^{70\ K}_{SME}(T)$, respectively, matches very well the DME curve $\Delta\rho^{70\ K,60\ K}_{DME}(T)$, as illustrated in Fig. 3(a). For another example, we reduced t_a of the pause at 60 K to 0.5 h in both the SME and the DME experiments [Fig. 3(b)]. In the $\Delta\rho^{70\ K,60\ K}_{DME}(T)$ curve, the memory maximum near 60 K is reduced, the memory at 70 K now emerges as a cusp, and most importantly we again observed that the superposition of two SME's gives the corresponding DME. Unambiguously, the system can memorize multiple events separately created on a single cooling and store them without interference—a behavior that has been well observed in magnetic glasses.[25,26,29,30]

The use of temperature as the only parameter to vary the dynamics of the system allows probing the system by its original dynamics. The observed nonequilibrium behaviors of resistance bear striking resemblances to the dynamic characteristics of magnetic glasses. The resistance keeps relaxing toward equilibrium in such a long period of time that could go beyond the laboratory time scale even in a constantly stabilized condition. After being "aged" at the pauses during cooling, the system responds differently on reheating, demonstrating a clear age-dependent behavior. Furthermore, the temperature memory effect, an inherent characteristic of magnetic glasses, is also observed. Since the resistive glassy behaviors are observed only in the FM state, they must have a magnetic origin. The insulating behavior in the FM state

suggests that the sample is not a pure DE ferromagnet but probably a separated system consisting of two competing phases: DE FM metallic-conducting domains separated by a non-FM insulating matrix. Low temperatures or high magnetic fields both favor the DE interaction and expand the FM domains at the expense of the non-FM insulating matrix. During the pause below T_c, the FM domains would evolve with time by polarizing the spins surrounding to expand the conducting regions. On the other hand, thermal activation helps the domain moments relax toward directions which are energetically favored by their randomly distributed local anisotropy, therefore increasing the spin scattering of electrons traveling between domains. The domain growth seems to be dominant at low temperatures, resulting in a downward resistivity relaxation (Fig. 2). In contrast, magnetic moments relax faster at higher temperatures, overcoming the domain growth process at temperatures close to T_c and therefore producing an upward resistivity relaxation. In the memory experiments, $\Delta\rho(T)$ approaches zero only at sufficiently high temperatures far above T_a, at which there is effectively no difference in domain sizes between the memory and the reference configurations.

We adopt the Néel relaxation law[32] to qualitatively describe the freezing of FM domains, $\tau=\tau_0 \exp(E_a/k_BT)$, where E_a is the anisotropy energy that is proportional to the domain size, k_B is the Boltzmann constant, and τ and τ_0 are the relaxation and microscopic relaxation times, respectively. Lowering temperature leads to an exponential increase in τ, causing the domains to become more deeply frozen. One of the key ingredients of the temperature memory effect is the freezing of magnetic moments in random directions that preserves the aged magnetic configuration when cooling is resumed after the pause. The frozen moments would still relax but with very much smaller rates at lower temperatures. Upon reheating, the melting of the aged configuration returns the system to the state without aging above T_a, exhibiting the observed memory effect. Since after the pause the magnetic moments relaxed into directions with higher energy barriers $[k_BT_a \ln(t_a/\tau_0)$, according to the Néel law] than k_BT_a, higher temperatures are then required to remove them from the freezing directions. This explains why the maximum of $\Delta\rho(T)$ is always at a higher temperature than T_a. In a real system, there always exist wide distributions of τ_0 and E_a. Magnetic moments of domains with $E_a \leq k_BT_a$ rotate freely due to thermal excitations, those with $E_a \gg k_BT_a$ are effectively frozen, and only those with $E_a \gtrsim k_BT_a$ contribute to the relaxation at T_a. This explains why we could observe a multiple temperature memory. Ideally, if $T_{a2} \ln(t_{a2}/\tau_0) < T_{a1}$, there could be no interference between the two aged configurations. In reality, upon cooling after the pause at T_{a1}, a finite cooling rate would allow the aged configuration to continue relaxing (although very slowly) at immediate temperature range below T_{a1}, the two memories are therefore completely separated only with $T_{a2} \ln(t_{a2}/\tau_0) \ll T_{a1}$.

In order to examine the influence of magnetic field on the memory effect, a magnetic field H_a was turned on during the pause. Right after the aging time t_a, H_a was removed and the cooling was immediately resumed. The SME $\Delta\rho(T)$ curves measured with different H_a's are presented in Fig. 4. The field is expected to favor the domain growth and therefore to increase the $\Delta\rho(T)$ maximum near T_a. However, the freezing of magnetic moments are also strongly affected. Instead of relaxing toward random directions, the magnetic moments are polarized and relax preferably toward the external field direction, establishing a configuration that is advantageous for the unfrozen domains to grow such that the domain growth during further cooling could effectively overwhelm the aged configuration previously established at T_a. We can see clearly in Fig. 4 that, while the maximum of the $\Delta\rho(T)$ curves is indeed raised with increasing H_a, it is significantly broadened and spreads toward lower temperatures. Apparently, higher H_a applied at T_a causes a stronger development of magnetic domains upon further cooling, which may interfere with the aged configuration pre-established at T_a. With $H_a=3$ kOe, the maximum of $\Delta\rho(T)$ is no longer defined, suggesting that the development of magnetic domains with decreasing temperature below T_a becomes entirely dominant.

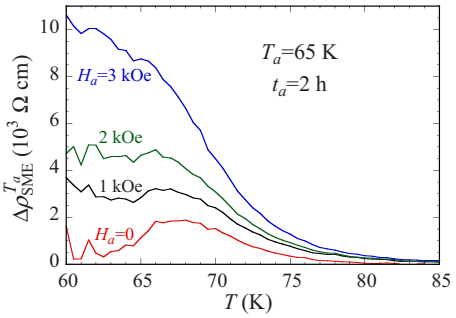

FIG. 4. (Color online) The influence of magnetic field on the nonequilibrium resistance dynamics. A magnetic field H_a is turned on during the pause at $T_a=65$ K upon cooling. The application of H_a causes a "crosstalk" between the memory established at T_a and the domain configurations developed during further cooling. The memory maximum in the $\Delta\rho^{65\ K}_{SME}(T)$ curve is unresolvable at $H_a=3$ kOe.

C. Temperature memory behavior of magnetization

Since the memory behavior of resistance is the result of thermomagnetic dynamic processes, it is natural to expect that similar effects can be observed in conventional magnetic measurements, even though the sample is in a ferromagnetic state. The results in Fig. 5 verify the temperature memory behavior of magnetization. With similar cooling procedures as those used for the transport measurements, depending on the probing field strength, the SME $M_{ZFC}(T)$ curve exhibits a "dip" or a "cusp" around T_a (insets of Fig. 5). For very small fields, the M_{ZFC} at a given temperature is contributed from FM domains having energy barriers lower than k_BT that can rotate toward the field direction. The freezing of magnetic moments that relaxed into higher energy barriers at T_a during the pause upon cooling is thus reflected by a dip in the memory curve lying below the reference curve. Melting these moments with increasing T above T_a drives the memory magnetization toward the reference one. The effect of larger domain sizes achieved by the pause is not exhibited because their moments are frozen in random directions. However, for high probing fields, the rotation of frozen mo-

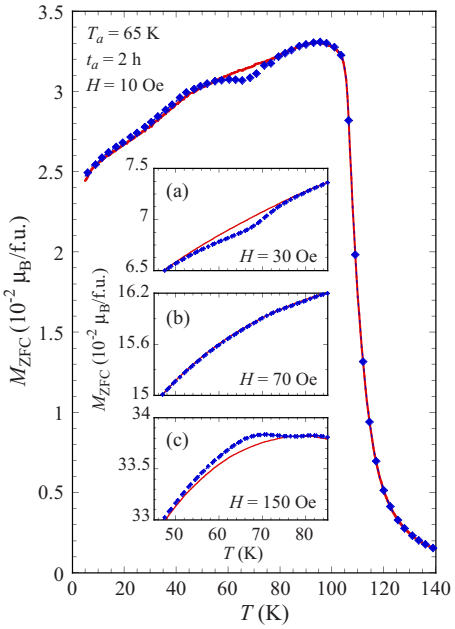

FIG. 5. (Color online) The temperature memory behavior observed on $M_{ZFC}(T)$. For the memory curves (symbols), the sample was zero-field-cooled from 300 to 5 K with a pause at T_a=65 K for t_a=2 h. For the reference curves (lines), the sample was cooled directly to 5 K. After the temperature had reached 5 K, a probing field H was immediately applied and $M_{ZFC}(T)$ was recorded on reheating. Main figure: H=10 Oe; insets (a), (b), and (c): H=30, 70, and 150 Oe, respectively. Sufficiently high probing fields can align the moments of the aged domains toward their direction, turning the memory dip lying below into a cusp lying above the reference curve.

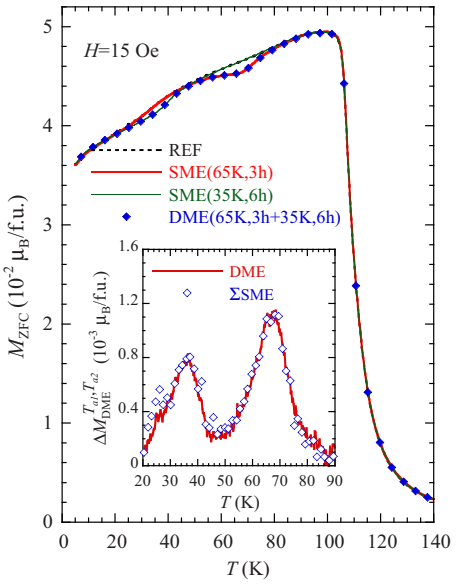

FIG. 6. (Color online) Double temperature memory observed on zero-field-cooled magnetization. Main figure: The reference curve, $M_{ref}(T)$ (dotted line), and the SME curves, $M_{SME}^{T_{a1}}(T)$ (bold line), and $M_{SME}^{T_{a2}}(T)$ (thin line), were measured using cooling procedures similar to those described in Fig. 5 with T_{a1}=65 K, t_{a1}=3 h, T_{a2}=35 K, t_{a2}=6 h, and H=15 Oe. The DME curve, $M_{DME}^{T_{a1},T_{a2}}(T)$ (solid diamond symbols), was measured under the same conditions as those for the SME curves but with cooling pauses at both T_{a1} and T_{a2}, showing two memory dips nearly identical to the corresponding SME ones. The inset shows the DME (line) as a combination of the two corresponding SME's (symbols), $\Delta M_{DME}^{T_{a1},T_{a2}}(T) = \Delta M_{SME}^{T_{a1}}(T) + \Delta M_{SME}^{T_{a2}}(T)$, where $\Delta M_{SME}^{T_a}(T) = M_{ref}(T) - M_{SME}^{T_a}(T)$ and $\Delta M_{DME}^{T_{a1},T_{a2}}(T) = M_{ref}(T) - M_{DME}^{T_{a1},T_{a2}}(T)$.

ments toward the field direction becomes significant; the larger FM domain sizes in the memory configuration (than in the corresponding reference one) give extra contributions to the magnetization. As a result, with increasing probing field, the memory dip gradually shallows and develops into a cusp lying above the reference curve. This influence of magnetic field on the memory behavior is thus in agreement with the picture of coexisting domain growth and magnetic freezing.

Figure 6 presents a double temperature memory observed in $M_{ZFC}(T)$ curves in comparison with the corresponding single temperature memories. In these experiments, temperature pauses were made at T_{a1}=65 K for t_{a1}=3 h and T_{a2}=35 K for t_{a2}=6 h during cooling and $M_{ZFC}(T)$ was then measured on heating in a small probing field H=15 Oe. The SME curves, $M_{SME}^{T_{a1}}(T)$ and $M_{SME}^{T_{a2}}(T)$, exhibit memory dips at T_{a1} and T_{a2}, respectively. Although the pause at T_{a2} is twice longer than that at T_{a1}, the dip at T_{a2} is significantly shallower since the magnetic moments relax slower at lower temperatures. Notably, this is in complete contrast to the results in Fig. 2, where the $\Delta\rho_{SME}^{T_a}(T)$ maximum is larger at a lower T_a. These distinguishable features are indeed consistent with our previous discussion that the FM domain growth, which reduced resistance and caused the memory maximum in the $\Delta\rho_{SME}^{Ta}(T)$ curves, is stronger with lowering T_a but has insignificant contribution to M_{ZFC} in a low probing field due to the random orientation of the frozen domain moments. On the other hand, the freezing of domain moments, while directly influencing the memory behavior of magnetization, has lesser influence on the resistivity. As clear evidence for the double memory effect, the corresponding $M_{DME}^{T_{a1},T_{a2}}(T)$ curve has a two-dip structure with the dips almost coinciding with those of the corresponding SME curves at T_{a1} and T_{a2}. This indicates that the pause at T_{a2} has insignificant influence on the aged state already established at T_{a1} and vice versa, effectively leading to almost no interference between the two memories. Accordingly, as shown in the inset of Fig. 6, the reduced DME magnetization curve, $\Delta M_{DME}^{T_{a1},T_{a2}}(T) = M_{ref}(T) - M_{DME}^{T_{a1},T_{a2}}(T)$, shows two memory peaks at temperatures near (but slightly higher than) T_{a1} and T_{a2}. These peaks almost coincide with those of the reduced SME magnetization curves, $\Delta M_{SME}^{T_a}(T) = M_{ref}(T) - M_{SME}^{T_a}(T)$ (omitted for clarity). Similar to the results in Fig. 3, the summation of the two reduced SME magnetization curves, $\Delta M_{SME}^{T_{a1}}(T) + \Delta M_{SME}^{T_{a2}}(T)$, also matches very well the $\Delta M_{DME}^{T_{a1},T_{a2}}(T)$ curve, unequivocally indicating that a multiple memory can be combined by the corresponding single memories.

We emphasize here that, although the glassiness observed for the present manganite system is apparently very similar to that of a spin glass, the underlying physics may be different. For spin glasses, nonequilibrium dynamic behaviors such as magnetic aging and memory have been successfully explained in terms of "droplet excitations" described by

Fisher and Huse.[33,34] However, the droplet model was proposed for pure Ising spin glasses, while our sample is a phase separated ferromagnet and droplet excitations as well as nonequilibrium dynamics are not supposed to exist in the ferromagnetic domains. On the other hand, a pure spin-glass or cluster-glass model can explain only the magnetic glassy behavior but is not adequate for understanding the resistive glassiness. It is important to note that magnetic freezing during the pause that causes a dip in low-field M_{ZFC} cannot explain the memory maximum of $\Delta\rho$ and its enlargement with decreasing temperature. For the resistive glassy behavior, a phase evolution (or domain growth) should be involved; our model therefore necessarily combines both these crucial factors: magnetic freezing and phase evolution. In our discussion, we have ignored the domain morphology which might contribute a term to the domain anisotropy. This contribution from domain morphology would be very small (compared to the contributions from crystalline anisotropy and domain size) and is not accounted for in the Néel relaxation law.

IV. CONCLUSION

Nonequilibrium dynamic behaviors such as long-time relaxation, aging, and temperature memory of both resistivity and magnetization have been revealed in the insulator ferromagnet $La_{0.7}Ca_{0.3}Mn_{0.925}Ti_{0.075}O_3$. The glassy transport has a very close association with the magnetic glassiness and appears to be magnetically related. These results can be qualitatively explained in terms of two competing thermodynamic processes: domain growth and magnetic freezing. The results of our dynamical study evidence the presence of phase separation and strong correlation between magnetism and electrical transport in the CMR perovskite manganite. We propose that resistive glassiness is a common character of mixed-valence perovskite manganites as a direct result of both electronic and magnetic phase separation. This nonequilibrium dynamics may be found profound in systems where there exists a strong competition between conducting and insulating phases, most likely near the metal-insulator transition with doping. Since the temperature memory behavior of resistance is associated with the freezing of magnetic domains, it is expected to be observable in the manganite insulators where FM metallic domains are embedded in the non-FM insulating matrix.

ACKNOWLEDGMENTS

This work was performed using the facilities of the State Key Laboratories (IMS, VAST). The authors thank N. C. Thuan for the updated PPMS measurements.

*daonhnam@yahoo.com

[1] A. Vaknin, Z. Ovadyahu, and M. Pollak, Phys. Rev. B **65**, 134208 (2002).
[2] V. Orlyanchik and Z. Ovadyahu, Phys. Rev. B **75**, 174205 (2007).
[3] J. Jaroszyński and D. Popović, Phys. Rev. Lett. **99**, 216401 (2007).
[4] S. Borini, L. Boarino, and G. Amato, Phys. Rev. B **75**, 165205 (2007).
[5] G. Martinez-Arizala, C. Christiansen, D. E. Grupp, N. Marković, A. M. Mack, and A. M. Goldman, Phys. Rev. B **57**, R670 (1998).
[6] E. Bielejec and W. Wu, Phys. Rev. Lett. **87**, 256601 (2001).
[7] T. Grenet, J. Delahaye, M. Sabra, and F. Gay, Eur. Phys. J. B **56**, 183 (2007).
[8] M. Lee, P. Oikonomou, P. Segalova, T. F. Rosenbaum, A. F. Th. Hoekstra, and P. B. Littlewood, J. Phys.: Condens. Matter **17**, L439 (2005).
[9] M. Roy, J. F. Mitchell, and P. Schiffer, J. Appl. Phys. **87**, 5831 (2000).
[10] P. Levy, F. Parisi, L. Granja, E. Indelicato, and G. Polla, Phys. Rev. Lett. **89**, 137001 (2002).
[11] J. Tao, D. Niebieskikwiat, M. B. Salamon, and J. M. Zuo, Phys. Rev. Lett. **94**, 147206 (2005).
[12] K. De, S. Majumdar, and S. Giri, J. Appl. Phys. **101**, 103909 (2007).
[13] J. Wu, H. Zheng, J. F. Mitchell, and C. Leighton, Phys. Rev. B **73**, 020404(R) (2006).
[14] T. Kimura, Y. Tomioka, R. Kumai, Y. Okimoto, and Y. Tokura, Phys. Rev. Lett. **83**, 3940 (1999).
[15] A. Anane, J.-P. Renard, L. Reversat, C. Dupas, P. Veillet, M. Viret, L. Pinsard, and A. Revcolevschi, Phys. Rev. B **59**, 77 (1999).
[16] R. von Helmolt, J. Wecker, T. Lorenz, and K. Samwer, Appl. Phys. Lett. **67**, 2093 (1995).
[17] D. Casa, B. Keimer, M. v. Zimmermann, J. P. Hill, H. U. Habermeier, and F. S. Razavi, Phys. Rev. B **64**, 100404(R) (2001).
[18] X. J. Chen, H.-U. Habermeier, and C. C. Almasan, Phys. Rev. B **68**, 132407 (2003).
[19] A. Bhattacharya, M. Eblen-Zayas, N. E. Staley, A. L. Kobrinskii, and A. M. Goldman, Phys. Rev. B **72**, 132406 (2005).
[20] R. M. Kusters, J. Singleton, D. A. Keen, R. Mcgreevy, and W. Hayes, Physica B (Amsterdam) **155**, 362 (1989).
[21] S. Jin, T. H. Tiefel, M. McCormac, R. A. Fastnacht, R. Ramesh, and L. H. Chen, Science **264**, 413 (1994).
[22] C. Zener, Phys. Rev. **82**, 403 (1951).
[23] X. Liu, X. Xu, and Y. Zhang, Phys. Rev. B **62**, 15112 (2000).
[24] D. N. H. Nam, L. V. Bau, N. V. Khiem, N. V. Dai, L. V. Hong, N. X. Phuc, R. S. Newrock, and P. Nordblad, Phys. Rev. B **73**, 184430 (2006).
[25] K. Jonason, E. Vincent, J. Hammann, J. P. Bouchaud, and P. Nordblad, Phys. Rev. Lett. **81**, 3243 (1998).
[26] T. Jonsson, K. Jonason, and P. Nordblad, Phys. Rev. B **59**, 9402 (1999).
[27] R. Mathieu, P. Jönsson, D. N. H. Nam, and P. Nordblad, Phys. Rev. B **63**, 092401 (2001).
[28] D. N. H. Nam, K. Jonason, P. Nordblad, N. V. Khiem, and N. X. Phuc, Phys. Rev. B **59**, 4189 (1999).

[29] D. N. H. Nam, R. Mathieu, P. Nordblad, N. V. Khiem, and N. X. Phuc, Phys. Rev. B **62**, 8989 (2000).
[30] R. Mathieu, P. Nordblad, D. N. H. Nam, N. X. Phuc, and N. V. Khiem, Phys. Rev. B **63**, 174405 (2001).
[31] D. N. H. Nam, R. Mathieu, P. Nordblad, N. V. Khiem, and N. X. Phuc, J. Magn. Magn. Mater. **226-230**, 1340 (2001).
[32] L. Néel, Ann. Geophys. (C.N.R.S.) **5**, 99 (1949).
[33] D. S. Fisher and D. A. Huse, Phys. Rev. B **38**, 373 (1988).
[34] D. S. Fisher and D. A. Huse, Phys. Rev. B **38**, 386 (1988).